

# Reaction of Unconjugated Dienes with $[\text{Fe}(\text{R}_2\text{P}(\text{CH}_2)_n\text{PR}_2)]$ Species<sup>†</sup>

S. Geier, R. Goddard, S. Holle, P. W. Jolly,\* C. Krüger, and F. Lutz

Max-Planck-Institut für Kohlenforschung, D-45466 Mülheim an der Ruhr, Germany

Received November 27, 1996<sup>⊗</sup>

The effect of varying the bidentate ligand upon the reaction of unconjugated dienes with  $(\text{R}_2\text{P}(\text{CH}_2)_n\text{PR}_2)\text{Fe}^0$  species has been investigated. Depending upon the nature of the substituents at phosphorus and upon the length of the hydrocarbon chain joining the phosphorus atoms, either  $(\eta^2:\eta^2\text{-diene})\text{Fe}(\text{R}_2\text{P}(\text{CH}_2)_n\text{PR}_2)$  or  $(\eta^5\text{-dienyl})\text{Fe}(\text{R}_2\text{P}(\text{CH}_2)_n\text{PR}_2)\text{H}$  species are formed. Extended Hückel MO-calculations have been used to assess the importance of electronic factors in influencing the course of reaction, and it can be shown that distortion of the tetrahedral geometry of the (diene)Fe species causes a destabilization.

## Introduction

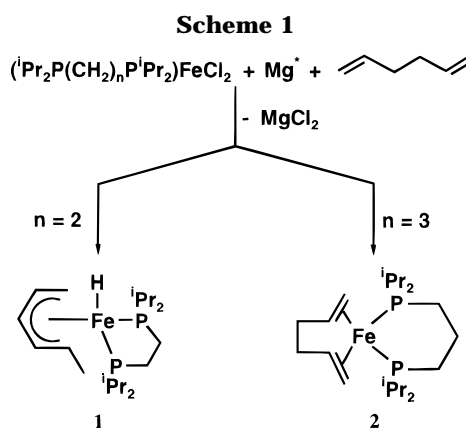
Recently we reported that the structure of the compounds formed upon reacting  $\text{Fe}(\text{iPr}_2\text{P}(\text{CH}_2)_n\text{P}^i\text{iPr}_2)\text{Cl}_2$  ( $n = 1-3$ ) with active Mg and acyclic dienes depends upon the nature of the diene and the length of the methylene chain joining the two P atoms of the bidentate ligand.<sup>1</sup> For example, 1,5-hexadiene reacts with the  $\text{Fe}(\text{iPr}_2\text{P}(\text{CH}_2)_n\text{P}^i\text{iPr}_2)$  fragment to give the  $(\eta^5\text{-2,4-hexadien-1-yl})\text{iron hydride}$  **1** in the presence of the ethylene-bridged ligand and to give the  $(\eta^2:\eta^2\text{-1,5-hexadiene})\text{Fe}$  species **2** in the presence of the trimethylene-bridged ligand (Scheme 1). Furthermore, neither compound shows any tendency to interconvert below the decomposition temperature.

We have now extended our investigations to include other substituted diphosphines and unconjugated dienes. Here we report the synthetic results and discuss the effect of electronic factors upon the course of reaction. In a subsequent publication we will present a theoretical interpretation on the basis of molecular modeling.

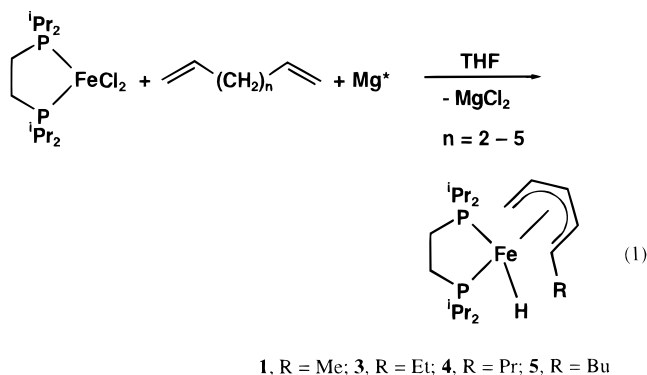
## Results and Discussion

The reactions investigated fall into three groups, which will be discussed separately: (1) the reaction of  $(\text{iPr}_2\text{PC}_2\text{H}_4\text{P}^i\text{iPr}_2)\text{Fe}^0$  species with a variety of nonconjugated dienes, (2) the reaction of the same dienes with the  $(\text{iPr}_2\text{PC}_3\text{H}_6\text{P}^i\text{iPr}_2)\text{Fe}^0$  species, and (3) the reaction of 1,5-hexadiene with a series of  $\text{R}_2\text{P}(\text{CH}_2)_n\text{PR}_2$ -stabilized iron species as well as with  $(\text{Et}_3\text{P})_2\text{Fe}^0$ . In all three cases, the (bidentate phosphine)Fe<sup>0</sup> fragment was prepared in situ by reducing  $\text{FeCl}_2 \cdot n\text{THF}$  with active Mg (prepared by vacuum pyrolysis of  $\text{MgH}_2$ )<sup>2</sup> in the presence of the ligand at low temperature.

**Reaction of  $(\text{iPr}_2\text{PC}_2\text{H}_4\text{P}^i\text{iPr}_2)\text{Fe}^0$  with Nonconjugated Dienes.** 1,5-Hexadiene, 1,6-heptadiene, 1,7-octadiene, and 1,8-nonadiene all react with the bis-



(diisopropylphosphino)ethane-stabilized zerovalent-iron fragment to give  $(\eta^5\text{-dienyl})\text{Fe}$ -hydrido complexes (**1** and **3**–**5**; eq 1) as yellow to orange solids. The yield



decreases with the separation of the double bonds, being ca. 70% for 1,5-hexadiene and ca. 20% for 1,8-nonadiene. The propyl-substituted compound **4** could not be isolated analytically pure and has been identified by comparison of the spectroscopic data (<sup>31</sup>P NMR  $\delta$  119.4, 113.7; <sup>1</sup>H NMR  $\delta$ (FeH) = 18.22,  $J(\text{P},\text{H}) = 73.0$  Hz) with those for **1**, **3** and **5**. In contrast, no stable product could be isolated in the presence of 1,4-pentadiene ( $n = 1$ ), presumably because strain prevents the complexation of both double bonds to one metal center.

Compounds **3** and **5** have been identified by comparing the spectroscopic data with those for **1**, whose crystal structure has been confirmed by X-ray diffraction.<sup>1</sup> Of

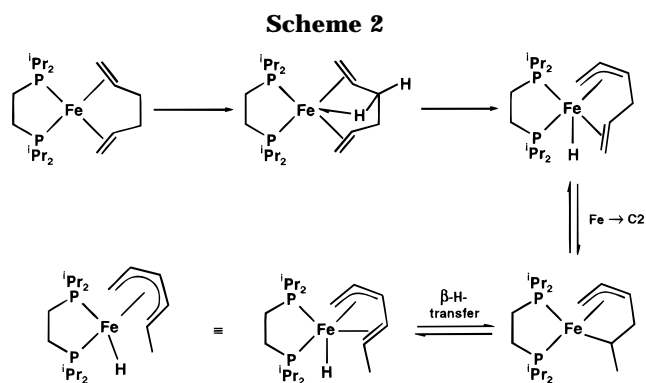
\* To whom correspondence should be addressed.

<sup>†</sup> Part of the doctoral thesis of S.G., submitted to the Ruhr-Universität Bochum in January 1996.

<sup>⊗</sup> Abstract published in *Advance ACS Abstracts*, March 15, 1997.

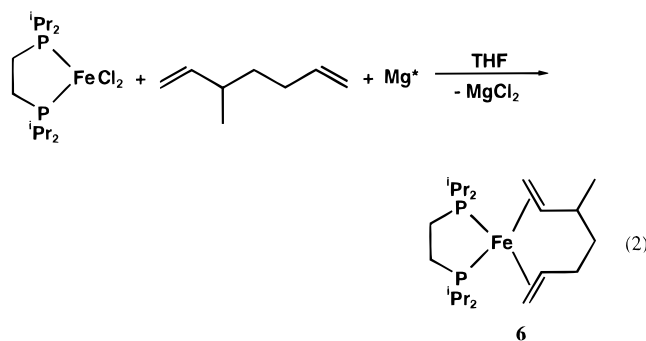
(1) Gabor, B.; Goddard, R.; Holle, S.; Jolly, P. W.; Krüger, C.; Mynott, R.; Wisniewski, S. *Z. Naturforsch.* **1995**, *50B*, 503.

(2) Bartmann, E.; Bogdanović, B.; Janke, N.; Liao, S.; Schlichte, K.; Spliethoff, B.; Treber, J.; Westeppe, U.; Wilczok, U. *Chem. Ber.* **1990**, *123*, 1517.



diagnostic use are the absorptions at ca.  $1900\text{ cm}^{-1}$  in the IR spectra and at ca.  $-18\text{ ppm}$  in the  $^1\text{H}$  NMR spectra, which we assign to the Fe–H moiety. Mechanistically relevant is the observation that, irrespective of the separation of the double bonds, the product invariably contains a dienylyl group substituted in the 5-position (and not, for example, in the 1,5-positions). The driving force for the reaction is presumably the formation of a stable 18-electron compound, and it is assumed to proceed by initial coordination of the diene to the metal atom followed by H-transfer from a methylene group to the metal and sequential Fe–H addition–elimination steps. This is illustrated in Scheme 2 for 1,5-hexadiene. The decrease in yield with increasing alkene separation is probably the result of the difference in the stability of the initial  $(\eta^2:\eta^2\text{-diene})\text{Fe}^0$  species and in the increasing importance of side reactions during the isomerization steps.

The suggested initial C–H activation shown above is supported by results with 3-methyl-1,6-heptadiene: the dark green, paramagnetic  $(\eta^2:\eta^2\text{-diene})\text{Fe}^0$  species **6** is formed in good yield (eq 2) and not a complex related to **3**. Furthermore, **6** shows no tendency to rearrange

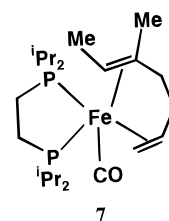


below the decomposition point ( $0\text{ }^\circ\text{C}$ ). Apparently the presence of a methyl group in the 3-position prevents the hydrocarbon chain joining the two double bonds from approaching the metal atom and suppresses further reaction.

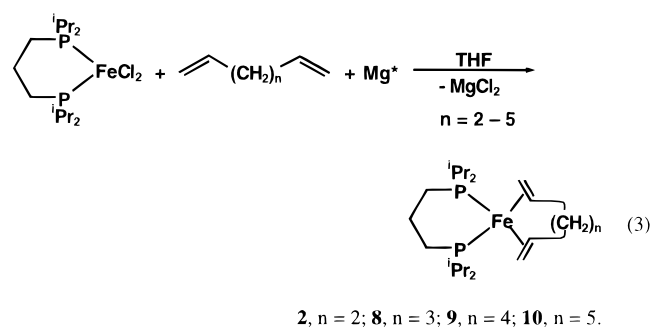
The structure of **6** has been established by a crystal structure determination. Although disorder in both the bidentate ligand and in the diene prevented refinement of the data ( $R > 10\%$ ), the tetrahedral environment around the metal atom and the conformation of the organic ligand could be confirmed. In addition, the mass spectrum of **6** contains fragments typical for 3-methyl-1,6-heptadiene.

Careful identification of **6** was necessary because the product of the further reaction with CO is a mixture of three diamagnetic adducts. The main component (46%)

is a compound (**7**) containing 5-methyl-1,5-heptadiene as the result of a CO-induced isomerization of the diene. The structure of **7** follows from the NMR spectroscopic data.



**Reaction of  $(i\text{Pr}_2\text{PC}_3\text{H}_6\text{P}i\text{Pr}_2)\text{Fe}^0$  with Nonconjugated Dienes.** The dienes mentioned above all react with the bis(diisopropylphosphino)propane-stabilized zerovalent-iron species to give the  $(\eta^2:\eta^2\text{-diene})\text{Fe}(i\text{Pr}_2\text{PC}_3\text{H}_6\text{P}i\text{Pr}_2)$  compounds **2** and **8–10** (eq 3) as dark green paramagnetic compounds. The compounds decompose



above  $-10$  to  $0\text{ }^\circ\text{C}$  without rearranging to the corresponding  $(\eta^5\text{-dienyl})\text{Fe-H}$  derivative.

The crystal structures of **2** and **8** have been established by X-ray diffraction. The hexadiene molecule in **2** was shown previously<sup>1</sup> to adopt two orientations at the metal which differ in the cisoid ( $C_s$ , local symmetry) arrangement (70% occupancy) or transoid ( $C_2$ , local symmetry) arrangement (30% occupancy) of the double bonds. The heptadiene molecule in **8** also adopts two arrangements (occupancy 75%:25%) but in contrast to **2** it is not possible to determine whether the diene occurs solely in the cisoid configuration with a different orientation at the metal atom (occupancy 100%) or as a mixture of cisoid and transoid arrangements (75%:25%). The molecular structure of the main conformer is shown in Figure 1 (minor component dashed), and selected structural data are listed in Table 1. The iron atom in **8** has a distorted-tetrahedral geometry: a decrease in the P–Fe–P angle from the tetrahedral value is accompanied by an increase in the D1–Fe–D2 angle (where D1 and D2 are the central points of the double bonds). The preferred chair conformation of the diene presumably reflects a more strain-free complexation, an effect which has also been noted for a number of zerovalent nickel–diene compounds.<sup>3,4</sup>

The iron atom in **2** and **8–10** is both coordinatively and electronically unsaturated, and a facile reaction with CO is observed. As discussed above for **7**, these reactions are probably accompanied by isomerization of the diene, and in all cases the  $^{31}\text{P}$  NMR spectra indicate

(3) Proft, B.; Pörschke, K. R.; Lutz, F.; Krüger, C. *Chem. Ber.* **1991**, *124*, 2667.

(4) Dreher, E.; Gabor, B.; Jolly, P. W.; Kopiske, C.; Krüger, C.; Limberg, A.; Mynott, R. *Organometallics* **1995**, *14*, 1893.

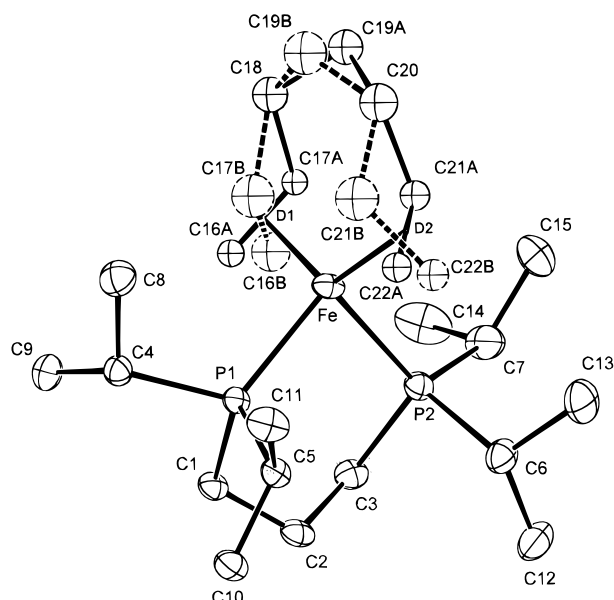


**Figure 1.** Molecular structure of  $(\eta^2:\eta^2\text{-}1,6\text{-heptadiene})\text{Fe}(\text{}^t\text{Pr}_2\text{PC}_3\text{H}_6\text{P}^t\text{Pr}_2)$  (**8**), showing the disorder in the heptadiene ligand (minor component (25%) represented by dashed lines). D1 and D2 are the midpoints of the C16A–C17A and C21A–C22A bonds.

**Table 1. Structural Data for  $(\eta^2:\eta^2\text{-}1,6\text{-C}_7\text{H}_{12})\text{Fe}(\text{}^t\text{Pr}_2\text{PC}_3\text{H}_6\text{P}^t\text{Pr}_2)$  (**8**)<sup>a</sup>**

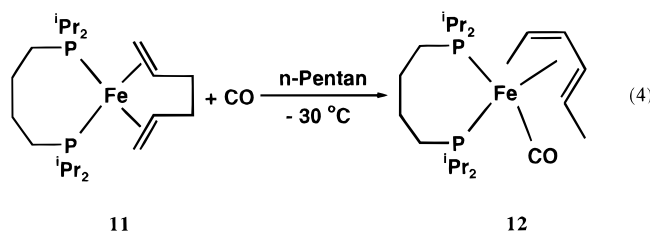
Bond Lengths (Å)			
Fe–P1	2.283(1)	Fe–P2	2.393(1)
Fe–C16A	2.109(3)	Fe–C17A	2.076(3)
Fe–C21A	2.066(4)	Fe–C22A	2.065(3)
C16A–C17A	1.424(4)	C21A–C22A	1.408(4)
C17A–C18	1.485(4)	C18–C19A	1.499(5)
C19A–C20	1.548(5)	C20–C21A	1.515(5)
P1–C1	1.847(3)	P2–C3	1.839(3)
C1–C2	1.527(4)	C2–C3	1.541(4)
P1–C4	1.885(3)	P1–C5	1.878(3)
P2–C6	1.867(3)	P2–C7	1.884(3)
Bond Angles (deg)			
P1–Fe–P2	92.6(4)	D1–Fe–D2	124.1
P1–Fe–D1	107.8	P1–Fe–D2	116.8
P2–Fe–D1	101.9	P2–Fe–D2	107.8
C16A–Fe–C17A	39.7(1)	C21A–Fe–C22A	38.9(1)
C16A–C17A–C18	122.2(3)	C22A–C21A–C20	117.9(3)
C17A–C18–C19A	115.3(3)	C18–C19A–C20	111.0(3)
C19A–C20–C21A	114.0(3)	Fe–P1–C1	113.9(1)
Fe–P2–C3	112.3(1)	P1–C1–C2	114.5(2)
P2–C3–C2	113.5(2)	C1–C2–C3	113.4(2)

<sup>a</sup> The data are from the isomer having 75% occupancy. ESDs are given in parentheses.

that a mixture of products is obtained. These have not been investigated further, since attempted displacement of the organic group by further reaction with CO under mild conditions was unsuccessful. The CO-induced isomerization of iron-complexed dienes is a well-known phenomenon, and examples relevant here are the reaction between iron pentacarbonyl and 1,5-hexadiene to give  $(\eta^4\text{-}1\text{-ethyl-, } 1,3\text{-butadiene})\text{Fe}(\text{CO})_3$ <sup>5</sup> and between  $(\eta^2:\eta^2\text{-}1,5\text{-cyclooctadiene})\text{Fe}(\text{}^t\text{Pr}_2\text{PC}_3\text{H}_6\text{P}^t\text{Pr}_2)$  and CO to give  $(\eta^4\text{-}1,3\text{-cyclooctadiene})\text{Fe}(\text{}^t\text{Pr}_2\text{PC}_3\text{H}_6\text{P}^t\text{Pr}_2)\text{CO}$ .<sup>6</sup>

**Reaction of  $(\text{R}_2\text{P}(\text{CH}_2)_n\text{PR}_2)\text{Fe}^0$  with 1,5-Hexadiene.** In addition to the reactions of the  $\text{}^i\text{Pr}_2\text{P}(\text{CH}_2)_n\text{P}^i\text{Pr}_2$ -stabilized species (where  $n = 2, 3$ ) with 1,5-

hexadiene (which lead to formation of **1** and **2**), we have also investigated the reactions where  $n = 1, 4$ , or  $5$ . In the presence of bis(diisopropylphosphino)methane ( $n = 1$ ), a dark black-brown reaction mixture is formed at low temperatures, while the reaction with bis(diisopropylphosphino)pentane ( $n = 5$ ) leads to the formation of a green compound which decomposes in solution even at  $-78^\circ\text{C}$  and could not be obtained analytically pure; therefore, it was not investigated further. The reaction in the presence of bis(diisopropylphosphino)butane was more successful, and the  $(\eta^2:\eta^2\text{-}1,5\text{-hexadiene})\text{Fe}$  complex **11** was obtained in good yield. This compound shows no tendency to react further below the decomposition point while, here again, the reaction with CO leads to isomerization of the diene and to the formation of a mixture of adducts, among which the  $(\eta^4\text{-}cis,trans\text{-}2,4\text{-hexadiene})\text{Fe}^0$  complex **12** was the main component (67%; <sup>31</sup>P NMR) (eq 4). The geometry of the diene in



**12** follows from a comparison of the <sup>13</sup>C NMR data with those of  $\text{CpCo}(\eta^4\text{-}cis,trans\text{-}2,4\text{-hexadiene})$ .<sup>7</sup>

Having varied the length of the hydrocarbon chain between the two phosphorus atoms, we next varied the substituent R in the  $(\text{R}_2\text{PC}_2\text{H}_4\text{PR}_2)\text{Fe}^0$  species. The reaction where R is isopropyl leads to the formation of **1**, and in addition, we have investigated reactions where the substituent is cyclopentyl (Cyp), cyclohexyl (Cy), *tert*-butyl, or ethyl. The course of reaction with 1,5-hexadiene was found to depend upon the nature of the substituent. In the case of the smallest substituent, ethyl, no reaction of the  $\text{Fe}(\text{Et}_2\text{PC}_2\text{H}_4\text{PET}_2)$  moiety with the diene was observed and the only product which could be isolated was  $\text{Fe}(\text{Et}_2\text{PC}_2\text{H}_4\text{PET}_2)_2$ .<sup>8</sup> In the other cases, an increase in the size of the substituent led to the suppression of C–H activation. Thus, whereas the product of the reaction in the presence of bis(dicyclopentylphosphino)ethane (R = Cyp) is  $(\eta^5\text{-}2,4\text{-hexadien-}1\text{-yl})\text{Fe}(\text{Cyp}_2\text{PC}_2\text{H}_4\text{PCyp}_2)\text{H}$ , in the presence of bis(dicyclohexylphosphino)ethane a mixture of the  $(\eta^5\text{-}2,4\text{-hexadien-}1\text{-yl})$ - and  $(\eta^2:\eta^2\text{-}1,5\text{-hexadiene})$ iron complexes is formed, while the bis(di-*tert*-butylphosphino)ethane-stabilized system leads to the formation of  $(\eta^2:\eta^2\text{-}1,5\text{-hexadiene})\text{Fe}(\text{}^t\text{Bu}_2\text{PC}_2\text{H}_4\text{P}^t\text{Bu}_2)$  (**13**) in 46% yield. Interestingly, although both types of compounds are formed in the reaction involving  $\text{Cy}_2\text{PC}_2\text{H}_4\text{PCy}_2$ , they do not interconvert and the (diene)Fe species decompose above  $0^\circ\text{C}$ .

The reaction of **13** with CO takes a different course from that described above for the related compounds **6** and **11**: substitution occurs, presumably due to the lability of the diene–iron bond (eq 5).

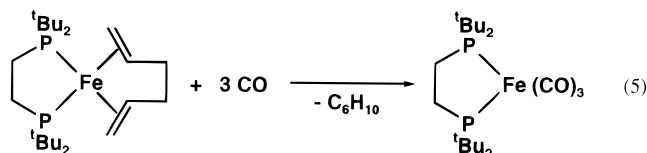
We have also investigated the reactions of the  $(\text{Et}_3\text{P})_2\text{Fe}^0$  fragment with 1,5-hexadiene:  $(\eta^2:\eta^2\text{-}1,5\text{-hexadiene})$ -

(5) Mahler, J. E.; Pettit, R. *J. Am. Chem. Soc.* **1963**, *85*, 3955.

(6) Frings, A.; Jonas, K. Unpublished results. Frings, A. Doctoral Thesis, Ruhr-Universität Bochum, 1988.

(7) Cibura, K. Doctoral dissertation, Ruhr-Universität Bochum, 1985. <sup>13</sup>C NMR (*d*<sub>8</sub>-toluene):  $\delta$  80.1 (C-3), 77.4 (C-4), 45.6 (C-2), 40.6 (C-5), 22.1 (C-6), 15.6 (C-1) (*cis,trans*-2,4-hexadiene).

(8) Field, L.; Baker, M. V. *Organometallics* **1986**, *5*, 821.



13

$Fe(PEt_3)_2$  (**14**) is formed in good yield. The crystal structure of **14** has been determined by X-ray diffraction, and the molecular structure is shown in Figure 2 and selected structural data in Table 2. In contrast to  $(\eta^2:\eta^2-1,5\text{-hexadiene})Fe(iPr_2PC_3H_6P^iPr_2)$  (**2**),<sup>1</sup> the diene chain in **14** is not disordered and adopts exclusively a cisoid ( $C_s$ , local symmetry) conformation. This conformation, which is the less preferred one in **2**, is presumably a result of the ca.  $12^\circ$  larger P–Fe–P angle. The ligands in **14** are arranged in an almost ideal tetrahedron around the metal atom, and the geometry resembles that observed for  $(\eta^2\text{-CH}_2=\text{CH}_2)_2Fe(PEt_3)_2$ .<sup>9</sup>

The experimental and structural data presented above suggest that the course of reaction between an unconjugated diene and a  $(R_2P(CH_2)_nPR_2)Fe^0$  species is controlled by both the steric requirements of the substituents at phosphorus and the bite angle (P–Fe–P) formed by the chelating bisphosphine with the metal: bulky substituents tend to encapsulate the metal atom, preventing the  $CH_2$  groups bridging the double bonds from approaching, while the accessibility of the metal atom is directly dependent upon the bite angle. These observations are summarized in Figure 3. In an attempt to give these effects a quantitative basis, we have made use of both molecular modeling and extended Hückel calculations. The latter are discussed below, while the application of molecular modeling will be presented in a later publication.

**Extended Hückel MO Calculations.** The results shown in Figure 4 confirm that the EHT calculations are able to qualitatively reproduce the d-orbital splitting expected for the pseudooctahedral geometry formed in  $(\eta^5\text{-}2,4\text{-hexadien-1-yl})Fe(iPr_2PC_2H_4P^iPr_2)H$  (**1**) as well as for the distorted-tetrahedral geometry found in  $(\eta^2:\eta^2\text{-}1,5\text{-hexadiene})Fe(iPr_2PC_3H_6P^iPr_2)$  (**2**) and  $(\eta^2\text{-CH}_2=\text{CH}_2)_2Fe(PEt_3)_2$ . The calculations were carried out by replacing the  $iPr$  groups by H atoms and the Et groups by Me groups, and the atomic positions were taken from the crystal structure data as described in the Experimental Section. No attempt was made to optimize the geometry.

The octahedral separation ( $\Delta E$ ) for **1** is 3.76 eV (338 nm). The tetrahedral separation is much smaller, and as a measure we have chosen the energy difference between the lowest and highest d orbitals and the following values are found: 2.06 eV (600 nm) for **2a**, 2.32 eV (535 nm) for **2b**, and 2.16 eV (574 nm) for the bis( $\eta^2$ -ethylene)Fe complex. The MO schemes correctly reflect the magnetic behavior of these complexes: the  $(\eta^5\text{-}2,4\text{-hexadien-1-yl})FeH$ -species (**1**) is formally an Fe(II) complex with six d electrons in the valence shell, and the low-spin configuration is confirmed by NMR spectroscopy, while the tetrahedral complexes are formally  $Fe^0$  species with eight d electrons and the resulting paramagnetism with two unpaired electrons is

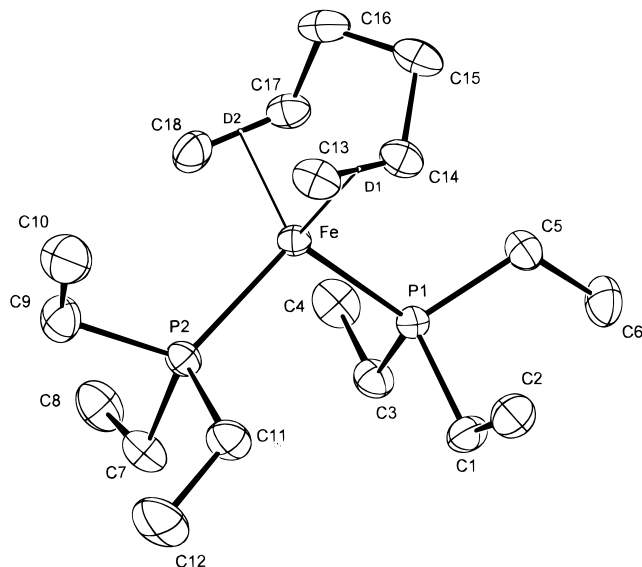


**Figure 2.** Molecular structure of  $(\eta^2:\eta^2\text{-}1,5\text{-hexadiene})Fe(PEt_3)_2$  (**14**). D1 and D2 are the midpoints of the C13–C14 and C17–C18 bonds.

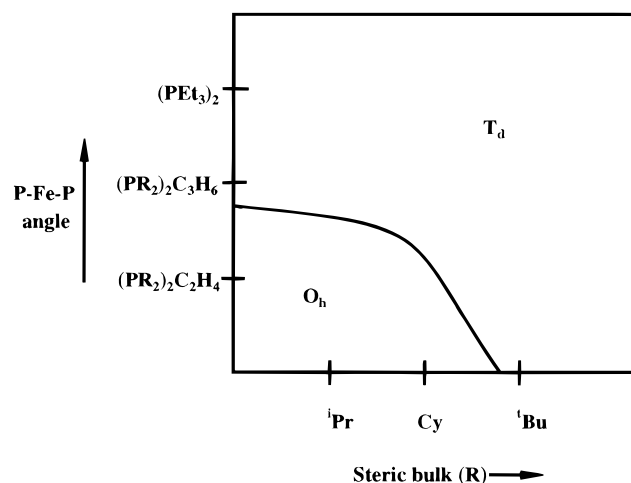


**Figure 3.** Schematic illustration of the products obtained when acyclic dienes react with  $Fe(R_2P(CH_2)_nPR_2)$  fragments in the examples studied ( $T_d$  = tetrahedral, **16e**  $(\eta^2:\eta^2\text{-}1,5\text{-hexadiene})Fe(R_2P(CH_2)_nPR_2)$ ;  $O_h$  = octahedral, **18e**  $(\eta^5\text{-}2,4\text{-hexadienyl})Fe(R_2P(CH_2)_nPR_2)H$ ).

**Table 2. Structural Data for  $(\eta^2:\eta^2\text{-}1,5\text{-C}_6\text{H}_{10})Fe(PEt_3)_2$  (**14**)<sup>a</sup>**

Bond Lengths (Å)			
Fe–P1	2.280(1)	Fe–P2	2.263(1)
Fe–C13	2.069(2)	Fe–C14	2.120(2)
Fe–C18	2.086(2)	Fe–C17	2.091(2)
C13–C14	1.406(3)	C18–C17	1.409(3)
C14–C15	1.523(3)	C15–C16	1.516(4)
C16–C17	1.517(3)		
Bond Angles (deg)			
P1–Fe–P2	105.1(1)	D1–Fe–D2	102.2
P1–Fe–D1	109.2	P1–Fe–D2	108.8
P2–Fe–D2	115.8	P2–Fe–D1	115.6
C13–Fe–C14	39.2(1)	C17–Fe–C18	39.4(1)
C13–C14–C15	121.9(2)	C18–C17–C16	122.3(2)
C14–C15–C16	109.1(2)	C15–C16–C17	109.5(2)

<sup>a</sup> Esd's are given in parentheses.

supported by the value of  $3.6 \mu_B$  determined experimentally for the magnetic susceptibility of  $(\eta^2:\eta^2\text{-}1,6\text{-heptadiene})Fe(iPr_2PC_3H_6P^iPr_2)$  (**8**).

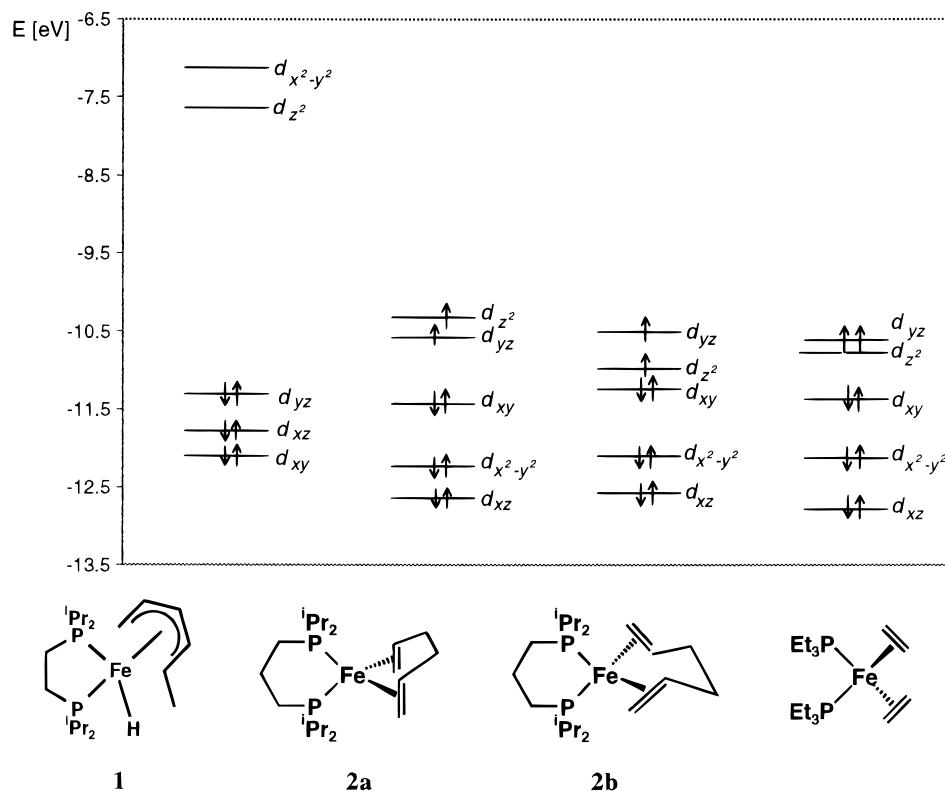


**Figure 4.** The d orbital separation in selected octahedral and tetrahedral iron complexes according to EHMO calculations.<sup>12</sup> Geometries are based upon the crystal structure data and the assignment of the MO's upon the largest contribution from the corresponding AO's (see Experimental Section for definition of coordinate system).

Inspection of the structural data available for the 16 tetrahedral iron complexes indicates that the introduction of methylene groups either between the two alkene groups or as bridging groups between the two P atoms leads to a *decrease* in the P–Fe–P angle from the near-tetrahedral value observed for  $(\eta^2\text{-CH}_2=\text{CH}_2)_2\text{Fe}(\text{PEt}_3)_2$  (P–Fe–P = 106.2°):<sup>9</sup>

$(\eta^2\text{-}\eta^2\text{-1,5-hexadiene})\text{Fe}(\text{PEt}_3)_2$ ( <b>14</b> )	105.1°
$(\eta^2\text{-}\eta^2\text{-1,5-hexadiene})\text{Fe}(\text{iPr}_2\text{PC}_3\text{H}_6\text{P}^i\text{Pr}_2)$ ( <b>2</b> )	95.0° <sup>1</sup>
$(\eta^2\text{-CH}_2=\text{CH}_2)_2\text{Fe}(\text{iPr}_2\text{PC}_3\text{H}_6\text{P}^i\text{Pr}_2)$	92.6° <sup>6</sup>

This distortion apparently becomes so large in going from a trimethylene-bridged to an ethylene-bridged bisphosphine that in the latter case the methylene groups in 1,5-hexadiene can interact with the metal and  $(\eta^5\text{-2,4-hexadien-1-yl})\text{Fe}(\text{iPr}_2\text{PC}_2\text{H}_4\text{P}^i\text{Pr}_2)\text{H}$  (**1**) is formed.

In order to determine what effect a change in the P–Fe–P angle has on the d-orbital splitting, we carried out a series of extended Hückel calculations on the hypothetical compound  $(\eta^2\text{-}\eta^2\text{-1,5-hexadiene})\text{Fe}(\text{PH}_3)_2$  with the diene arranged in a transoid ( $C_2$ ) conformation. The geometries were generated by molecular modeling using the crystal structure of  $(\eta^2\text{-}\eta^2\text{-1,5-hexadiene})\text{Fe}(\text{iPr}_2\text{PC}_3\text{H}_6\text{P}^i\text{Pr}_2)$  (**2**, *transoid*-hexadiene)<sup>1</sup> as the basis, and the P–Fe–P angles were varied from 75 to 130° in steps of 5°. The resulting correlation of the P–Fe–P angle and the separation of the metal d orbitals ( $\Delta E$ , the separation between the highest and lowest d orbitals) is shown in Figure 5.

A broad minimum is observed between 95° and 105°, confirming that any distortion of a tetrahedral arrangement causes an increase in the separation of the d orbitals and an increase in the total energy of the system. An increase in the P–Fe–P angle will lead

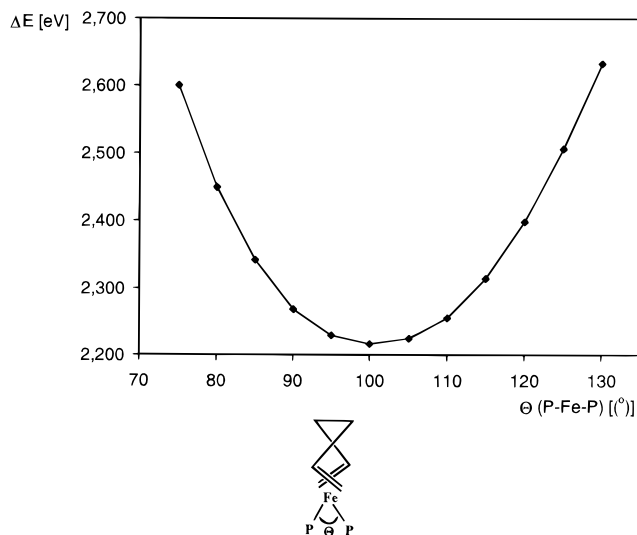


**Figure 5.** Correlation between the d orbital separation ( $\Delta E$ ) and the P–Fe–P angle ( $\theta$ ) in the hypothetical compound  $(\eta^2\text{-}\eta^2\text{-1,5-hexadiene})\text{Fe}(\text{PH}_3)_2$  ( $d^8$  system), in which the diene is arranged in a transoid ( $C_2$ ) conformation.

ultimately to a distorted-square-planar geometry in which the diene double bonds are rotated out of the plane. Decreasing the P–Fe–P angle leads to increased exposure of the metal orbitals.

To check the relevance of the curve shown in Figure 5, we have calculated the P–Fe–P angle for a series of model  $(\eta^2\text{-}\eta^2\text{-1,5-hexadiene})\text{Fe}(\text{iPr}_2\text{P}(\text{CH}_2)_n\text{P}^i\text{Pr}_2)$  ( $n = 1\text{--}5$ ) compounds (generated from valence force field calculations or minimized crystal structure data). The calculated d-orbital separations ( $\Delta E$ ) are listed in Table 3 and support the trend shown in Figure 5:  $\Delta E$  is a

**Table 3. Correlation between the Calculated P–Fe–P Angle for  $(\eta^2:\eta^2\text{-}1,5\text{-Hexadiene})\text{-Fe}(\text{Pr}_2\text{P}(\text{CH}_2)_n\text{P}(\text{Pr}_2))$  Complexes ( $n = 1\text{--}5$ ) and d Orbital Separation ( $\Delta E$ )**

$n$	$\theta(\text{P-Fe-P})$ , deg ( $R = \text{iPr}$ )	$\Delta E$ , eV ( $R = \text{H}$ )
1	74.1	2.63
2	85.1	2.58
3	94.8 (95.0 <sup>a</sup> )	2.36
4	98.7	2.31
$(\eta^2:\eta^2\text{-}1,5\text{-hexadiene})\text{Fe}(\text{PEt}_3)_2$	101.8 (102.3 <sup>a</sup> )	2.15
5	113.7	2.41

<sup>a</sup> Experimentally determine value.

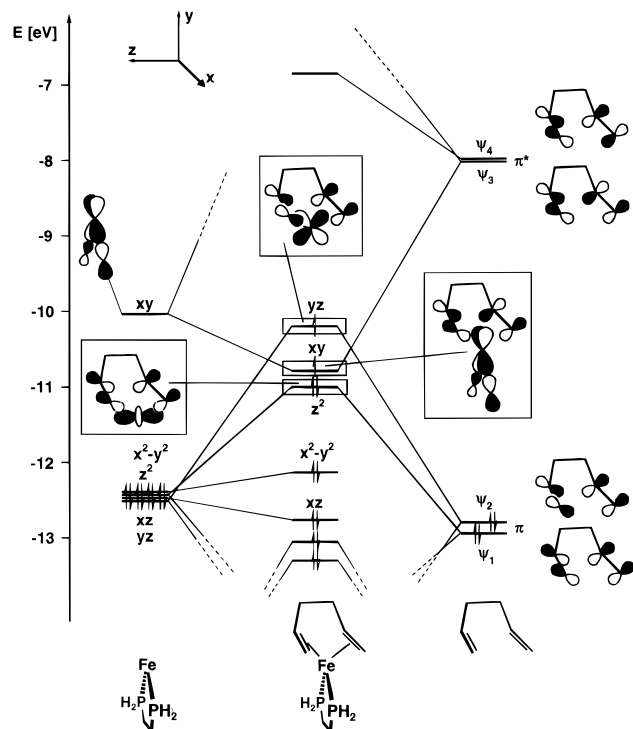


**Figure 6.** MO correlation scheme (EHT) for the hypothetical compound  $(\eta^2:\eta^2\text{-}1,5\text{-hexadiene})\text{Fe}(\text{H}_2\text{PC}_2\text{H}_4\text{PH}_2)$  with the hexadiene molecule in a *cisoid* conformation.

minimum close to the tetrahedral angle and increases on going to larger or smaller values.

The calculations are supported by the experimental results. Compounds such as  $(\eta^2:\eta^2\text{-}1,5\text{-hexadiene})\text{Fe}(\text{PEt}_3)_2$  (**14**) which have a near-tetrahedral P–Fe–P angle (and a low  $\Delta E$ ) are thermally stable and show no tendency to react further in spite of being 16e complexes. The introduction of bridging  $\text{CH}_2$  groups between the P atoms leads to a decrease in the P–Fe–P angle and destabilizes the compound ( $\Delta E$  increases). As one goes from  $\text{iPr}_2\text{PC}_3\text{H}_6\text{P}(\text{iPr})_2$  to  $\text{iPr}_2\text{PC}_2\text{H}_4\text{P}(\text{iPr})_2$ , the destabilization is apparently so large that the resulting energy increase is sufficient to compensate for a rehybridization of the metal d orbitals toward an octahedral field, leading to an increased exposure of the appropriate partially filled d orbitals, which are then able to interact with the  $\sigma^*$  C–H orbitals of the methylene bridge of the diene, and C–H cleavage can occur. The nature of this interaction is discussed below.

An MO correlation diagram for the hypothetical compound  $(\eta^2:\eta^2\text{-}1,5\text{-hexadiene})\text{Fe}(\text{H}_2\text{PC}_2\text{H}_4\text{PH}_2)$  is shown in Figure 6, which has been constructed with the aid of force field calculations and conformational analysis to generate an energetic minimum (the *cisoid* ( $C_2$ ) confor-

mation of the diene shown is actually 0.87 kcal/mol less stable than a crossed (*transoid*,  $C_2$ ) arrangement of the double bonds). The antibonding metal  $d_{xy}$  orbital interacts with the p orbitals of the P atom while the other metal d orbitals are essentially unchanged. The MO's of the hexadiene interact strongly with the  $d_{xy}$ -acceptor orbital and the  $d_{yz}$  and  $d_z^2$  orbitals. The d-orbital separation which results is that expected for a distorted-tetrahedral field, while the similarity in the energies of the  $d_{xy}$  and  $d_{yz}$  orbitals (0.6 eV = 13.8 kcal/mol) results in the species having two unpaired electrons (the small difference in energy between these orbitals is more than compensated by the spin-pairing energy, and a high-spin configuration results). Saillard and Hoffmann have applied EHT calculations to C–H activation in square-planar or distorted-square-planar complexes<sup>10</sup> and shown that a necessary prerequisite for oxidative addition of a C–H bond to a metal atom is a destabilization of an occupied metal d orbital (thus moving it closer in energy to  $\sigma^*$  of the C–H bond with which it interacts) and hybridization away from the fragment (thus providing better overlap with  $\sigma^*$  of C–H). The MO scheme shown in Figure 6 indicates that, in our tetrahedral complexes, the highest occupied orbitals also have a suitable energy and orientation to interact with the unfilled  $\sigma^*$  C–H MO's of the methylene groups. Furthermore, distortion from ideal tetrahedral geometry will lead to an increase in the energy of the  $d_{yz}$  orbital (see Figure 5) and result in better overlap with the  $\sigma^*$  C–H orbital.

## Conclusions

The results of the EHT calculations discussed here, and the molecular modeling which will be presented in a later publication, suggest that the two approaches complement each other. The course of the reaction between 1,5-hexadiene and the  $\text{Fe}(\text{R}_2\text{P}(\text{CH})_n\text{PR}_2)$  species is controlled in the first instance by steric factors, i.e. encapsulation of the metal by the bidentate ligand, and only when their significance is reduced can electronic factors become important and the reaction proceeds to the pseudo-octahedral  $(\eta^5\text{-}2,4\text{-hexadien-1-yl})\text{FeH}$  species.

The experimental and theoretical results indicate that, in the case of the  $\text{iPr}$ -substituted bisphosphine ligands, the limiting case occurs upon going from the trimethylene-bridged ligand ( $\text{iPr}_2\text{PC}_3\text{H}_6\text{P}(\text{iPr})_2$ ) to the ethylene-bridged ligand ( $\text{iPr}_2\text{PC}_2\text{H}_4\text{P}(\text{iPr})_2$ ). In the case of the ethylene-bridged  $\text{R}_2\text{PC}_2\text{H}_4\text{PR}_2$  ligands, the change from mainly steric to mainly electronic control occurs with  $\text{Cy}_2\text{PC}_2\text{H}_4\text{PCy}_2$ , since in the presence of this ligand both types of compounds, i.e.  $(\eta^2:\eta^2\text{-}1,5\text{-hexadiene})\text{Fe}(\text{Cy}_2\text{PC}_2\text{H}_4\text{PCy}_2)$  and  $(\eta^5\text{-}2,4\text{-hexadien-1-yl})\text{Fe}(\text{Cy}_2\text{PC}_2\text{H}_4\text{PCy}_2)\text{H}$ , are formed. The sterically less demanding  $\text{iPr}_2\text{PC}_2\text{H}_4\text{P}(\text{iPr})_2$  or sterically more demanding  $\text{tBu}_2\text{PC}_2\text{H}_4\text{P}(\text{tBu})_2$  ligands lead exclusively to the formation of  $(\eta^5\text{-}2,4\text{-hexadien-1-yl})\text{Fe}(\text{Pr}_2\text{PC}_2\text{H}_4\text{P}(\text{iPr})_2)\text{H}$  or  $(\eta^2:\eta^2\text{-}1,5\text{-hexadiene})\text{Fe}(\text{tBu}_2\text{PC}_2\text{H}_4\text{P}(\text{tBu})_2)$ .

## Experimental Section

The general experimental conditions and instrumentation have been described in an earlier publication.<sup>11</sup> The preparation of  $(\eta^5\text{-}2,4\text{-hexadien-1-yl})\text{Fe}(\text{Pr}_2\text{PC}_2\text{H}_4\text{P}(\text{iPr})_2)\text{H}$  (**1**) and  $(\eta^2:\eta^2\text{-}1,5\text{-hexadiene})\text{Fe}(\text{iPr}_2\text{PC}_3\text{H}_6\text{P}(\text{iPr})_2)$  (**2**) have been reported earlier.<sup>1</sup>

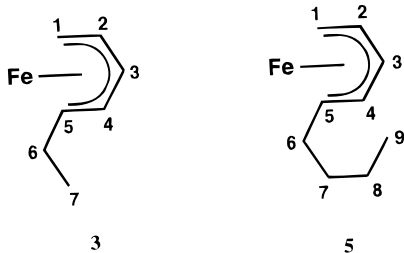
(10) Saillard, J.-Y.; Hoffmann, R. *J. Am. Chem. Soc.* **1984**, *106*, 2006.

(11) Gabor, B.; Holle, S.; Jolly, P. W.; Mynott, R. *J. Organomet. Chem.* **1994**, *466*, 201.

$\text{FeCl}_2 \cdot n\text{THF}$  was prepared by extracting anhydrous  $\text{FeCl}_2$  (Ventron) with THF in a Soxhlet apparatus, evaporating the extract, and drying the residue under high vacuum for 48 h. The composition was determined by elemental analysis. Activated Mg was prepared by the vacuum pyrolysis of  $\text{MgH}_2$ .<sup>2</sup>

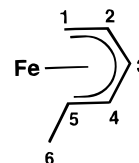
**1,5-Bis(diisopropylphosphino)pentane.** A solution of  $\text{Pr}_2\text{PLi}$  (10.39 g, 84 mmol) in THF (150 mL) was stirred, and a solution of 1,5-dibromopentane (10.35 g, 6 mL, 45 mmol) in THF (10 mL) was added slowly at 0 °C. The reaction mixture was warmed to room temperature, and the solvent was removed under vacuum. The resulting oily residue was taken up in hexane (150 mL) and filtered to remove LiBr. Evaporation of the solvent under high vacuum gave the compound as a viscous liquid. Yield: 8.33 g (65.2%). Anal. Calcd for  $\text{C}_{17}\text{H}_{38}\text{P}_2$ : C, 67.1; H, 12.6; P, 20.4. Found: C, 67.0; H, 12.7; P, 20.1. <sup>1</sup>H NMR ( $d_8$ -toluene):  $\delta$  1.70–0.94. <sup>13</sup>C NMR ( $d_8$ -toluene):  $\delta$  33.9/28.6/22.4 (t,  $\text{CH}_2$ ,  $J(\text{P},\text{C}) = 11.6/19.2/19.2$ ), 23.9/20.4/19.2 (d/q/q, i- $\text{C}_3\text{H}_7$ ,  $J(\text{P},\text{C}) = 14.8/15.7/10.5$ ). <sup>31</sup>P NMR ( $d_8$ -toluene):  $\delta$  2.87 (s).

**( $\eta^5$ -2,4-Hexadien-1-yl)Fe( $\text{Pr}_2\text{PC}_2\text{H}_4\text{P}^i\text{Pr}_2$ )H (3).**  $\text{FeCl}_2 \cdot n\text{THF}$  ( $n = 1.43$ ; 0.72 g, 3.12 mmol) was suspended in THF (60 mL) and treated with bis(diisopropylphosphino)ethane (0.82 g, 0.98 mL, 3.12 mmol). The reaction mixture was stirred at room temperature for 1 h and cooled to –78 °C, and 1,6-heptadiene (0.30 g, 0.42 mL, 3.12 mmol) and active Mg (0.08 g, 3.29 mmol) were added. The reaction mixture was stirred for 24 h at –35 °C, the resulting yellow-brown suspension was evaporated to dryness at –30 °C, and the residue extracted with precooled pentane (200 mL) at –30 °C. The extract was evaporated to dryness at –35 °C, and the residue dissolved in precooled pentane (100 mL). The solution was concentrated to half its volume and cooled to –78 °C to give a red-brown solid which was recrystallized from pentane to give the compound as an orange powder, which was washed with a small amount of precooled pentane and dried under high vacuum. Further product was obtained by concentrating the mother liquor. Yield: 0.28 g (22%). Anal. Calcd for  $\text{C}_{21}\text{H}_{44}\text{FeP}_2$ : C, 60.9; H, 10.7; Fe, 13.5; P, 15.0. Found: C, 61.0; H, 10.6; Fe, 13.6; P, 14.9. IR (KBr):  $\nu(\text{FeH})$  1850 m. MS (60 °C):  $m/e$  414 ( $\text{M}^+$ ), 318 ( $\text{M}^+ - \text{C}_7\text{H}_{12}$ ). <sup>1</sup>H NMR ( $d_8$ -toluene, –30 °C):  $\delta$  5.35 (br, H-3), 4.96 (br, H-4), 4.16 (br, H-2), 2.93 (br, H-5), 2.43 (br, H-<sub>1syn</sub>), –0.09 (br, H-<sub>1anti</sub>), –18.18 (dd, Fe–H,  $J(\text{P},\text{H}) = 72.0$ ). <sup>13</sup>C NMR ( $d_8$ -toluene, –30 °C):  $\delta$  92.4 (C-4), 90.6 (C-2), 80.1 (C-3), 65.4 (C-5), 48.4 (C-1), 31.7 (C-6). <sup>31</sup>P NMR ( $d_8$ -toluene, –30 °C):  $\delta$  119.6, 113.5 (numbering scheme shown below).



**( $\eta^5$ -2,4-Nonadien-1-yl)Fe( $\text{Pr}_2\text{PC}_2\text{H}_4\text{P}^i\text{Pr}_2$ )H (5).** Prepared as described above by reacting  $\text{FeCl}_2 \cdot n\text{THF}$  ( $n = 1.43$ ) with bis(diisopropylphosphino)ethane, 1,8-nonadiene, and active Mg in THF at –35 °C. The compound was isolated as a yellow-brown powder. Yield: 18.7%. Anal. Calcd for  $\text{C}_{23}\text{H}_{48}\text{FeP}_2$ : C, 62.4; H, 10.9; Fe, 12.6; P, 14.0. Found: C, 62.5; H, 10.9; Fe, 12.5; P, 13.9. IR (KBr):  $\nu(\text{FeH})$  1890 m. MS (60 °C):  $m/e$  442 ( $\text{M}^+$ ), 318 ( $\text{M}^+ - \text{C}_9\text{H}_{16}$ ). <sup>1</sup>H NMR ( $d_8$ -toluene, –30 °C):  $\delta$  5.37 (br, H-3), 5.02 (br, H-4), 4.17 (br, H-2), 2.47 (br, H-5), 2.02 (br, H-<sub>1syn</sub>), –0.06 (br, H-<sub>1anti</sub>), –18.17 (dd, FeH,  $J(\text{P},\text{H}) = 72.2$ ). <sup>13</sup>C NMR ( $d_8$ -toluene, –30 °C):  $\delta$  92.9 (C-4), 90.6 (C-2), 79.9 (C-3), 63.3 (C-5), 48.5 (C-1), 38.3 (C-6), 37.5 (C-7), 22.9 (C-8), 14.4 (C-9). <sup>31</sup>P NMR ( $d_8$ -toluene, –30 °C):  $\delta$  119.8, 113.9,  $J(\text{P},\text{P}) = 36.0$  (numbering scheme shown above).

**( $\eta^5$ -2,4-Hexadien-1-yl)Fe( $\text{Cyp}_2\text{PC}_2\text{H}_4\text{PCyp}_2$ )H** was prepared as described above by reacting  $\text{FeCl}_2 \cdot n\text{THF}$  ( $n = 1.5$ ) with bis(dicyclopentylphosphino)ethane, 1,5-hexadiene, and active Mg in THF at –35 °C. The compound is a yellow solid which decomposes above 0 °C. Yield: 39%. Anal. Calcd for  $\text{C}_{28}\text{H}_{50}\text{FeP}_2$ : C, 66.7; H, 10.0; Fe, 11.1; P, 12.3. Found: C, 64.9; H, 9.8; Fe, 10.7; P, 11.4. IR (KBr):  $\nu(\text{FeH})$  1875 m. MS (70 °C):  $m/e$  504 ( $\text{M}^+$ ), 500 ( $\text{M}^+ - 4\text{H}$ ), 418 ( $\text{M}^+ - 4\text{H}/\text{C}_6\text{H}_{10}$ ), 350. <sup>1</sup>H NMR ( $d_8$ -toluene, –30 °C):  $\delta$  5.42 (br, H-3), 5.10 (br, H-4), 4.25 (br, H-2), 2.56 (br, H-5), 2.43 (br, H-<sub>1syn</sub>), –0.20 (br, H-<sub>1anti</sub>), –18.02 (dd, FeH,  $J(\text{P},\text{H}) = 72.5$ ). <sup>13</sup>C NMR ( $d_8$ -toluene, –30 °C):  $\delta$  93.3 (C-4), 90.5 (C-2), 80.4 (C-3), 56.5 (C-5),  $J(\text{P},\text{C}) = 6.3/9.9$ , 46.1 (C-1),  $J(\text{P},\text{C}) = 10.1$ , 22.8 (C-6). <sup>31</sup>P NMR ( $d_8$ -toluene, –30 °C):  $\delta$  111.1, 109.5 (numbering scheme shown below).



**( $\eta^5$ -2,4-Hexadien-1-yl)Fe( $\text{Cy}_2\text{PC}_2\text{H}_4\text{PCy}_2$ )H** was prepared as described above by reacting  $\text{FeCl}_2 \cdot n\text{THF}$  ( $n = 1.5$ ) with bis(dicyclohexylphosphino)ethane, 1,5-hexadiene, and active Mg in THF at –35 °C. The reaction leads to the formation of a small amount of a green compound, which is presumably ( $\eta^2$ - $\eta^2$ -1,5-hexadiene)Fe( $\text{Cy}_2\text{PC}_2\text{H}_4\text{PCy}_2$ ), and the title compound, which is formed as a yellow-brown solid that decomposes rapidly above ca. 0 °C. Yield: 37.0%. Anal. Calcd for  $\text{C}_{32}\text{H}_{58}\text{FeP}_2$ : C, 68.6; H, 10.4; Fe, 10.0; P, 11.1. Found: C, 67.0; H, 10.3; Fe, 9.7; P, 10.8. IR (KBr):  $\nu(\text{FeH})$  1920 w. MS (90 °C):  $m/e$  560 ( $\text{M}^+$ ), 556 ( $\text{M}^+ - 4\text{H}$ ), 474 ( $\text{M}^+ - 4\text{H}/\text{C}_6\text{H}_{10}$ ). <sup>1</sup>H NMR ( $d_8$ -toluene, –30 °C):  $\delta$  5.44 (br, H-3), 5.09 (br, H-4), 4.32 (br, H-2), 2.63 (br, H-5), 2.42 (br, H-<sub>1syn</sub>), –0.09 (br, H-<sub>1anti</sub>), –18.20 (dd, FeH,  $J(\text{P},\text{H}) = 68.7$ ). <sup>13</sup>C NMR ( $d_8$ -toluene, –30 °C):  $\delta$  94.0 (C-4), 90.8 (C-2), 80.4 (C-3), 57.1 (C-5), 48.5 (C-1), 22.2 (C-6). <sup>31</sup>P NMR ( $d_8$ -toluene, –30 °C):  $\delta$  110.4, 103.7 (numbering scheme shown above).

**( $\eta^2$ : $\eta^2$ -1,6-Heptadiene)Fe( $\text{Pr}_2\text{PC}_3\text{H}_6\text{P}^i\text{Pr}_2$ ) (8).**  $\text{FeCl}_2 \cdot n\text{THF}$  ( $n = 1.38$ ; 0.87 g, 3.85 mmol) was suspended in THF (50 mL) at room temperature and stirred for 1 h with bis(diisopropylphosphino)propane (1.06 g, 1.23 mL, 3.85 mmol). The solution was cooled to –78 °C and treated with 1,6-heptadiene (0.37 g, 0.52 mL, 3.85 mmol) and active Mg (0.1 g, 4.11 mmol). The reaction mixture was stirred for 30 h at –40 °C to give a green suspension, which was evaporated to dryness at –35 °C under high vacuum. The residue was extracted with precooled pentane (200 mL) at –30 °C; the extract was filtered and concentrated to 60 mL. The solution was filtered, the residue was extracted with diethyl ether (40 mL), and the solutions combined and cooled to –78 °C. The resulting dark green precipitate was recrystallized from a pentane–diethylether mixture (1:1) at –30 to –78 °C to give the compound as dark green crystals. A second fraction was obtained from the mother liquor. The compound decomposes above 0 °C. Yield: 1.00 g (60.6%). Anal. Calcd for  $\text{C}_{22}\text{H}_{46}\text{FeP}_2$ : C, 61.7; H, 10.8; Fe, 13.0; P, 14.5. Found: C, 61.5; H, 10.9; Fe, 13.0; P, 14.5. IR (KBr):  $\nu$  1195 s, 1010 s. MS (50 °C):  $m/e$  442 ( $\text{M}^+$ ), 332 ( $\text{M}^+ - \text{C}_7\text{H}_{12}$ ). Magnetic susceptibility: 3.6  $\mu_B$ . Crystal structure determination: see Figure 1.

**( $\eta^2$ : $\eta^2$ -1,7-Octadiene)Fe( $\text{Pr}_2\text{PC}_3\text{H}_6\text{P}^i\text{Pr}_2$ ) (9)** was prepared as described above for **8** as a green, somewhat sticky solid by reacting  $\text{FeCl}_2 \cdot n\text{THF}$  ( $n = 1.38$ ) with the bidentate ligand, 1,7-octadiene, and active Mg in THF at –78 to –35 °C. The compound decomposes rapidly at temperatures above 0 °C. Yield: 20.1%. Anal. Calcd for  $\text{C}_{23}\text{H}_{48}\text{FeP}_2$ : C, 62.4; H, 10.9; Fe, 12.6; P, 14.0. Found: C, 62.6; H, 10.9; Fe, 12.5; P, 14.1. IR (KBr):  $\nu$  2955 s, 2925 s. MS (60 °C):  $m/e$  442 ( $\text{M}^+$ ), 332 ( $\text{M}^+ - \text{C}_8\text{H}_{14}$ ).

**( $\eta^2$ : $\eta^2$ -1,8-Nonadiene)Fe( $\text{Pr}_2\text{PC}_3\text{H}_6\text{P}^i\text{Pr}_2$ ) (10)** was prepared as described above for **8** as a green, sticky solid by

reacting  $FeCl_2 \cdot nTHF$  ( $n = 1.38$ ) with the bidentate ligand, 1,8-nonadiene, and active Mg in THF at  $-78$  to  $-35$  °C. The compound decomposes rapidly above  $-10$  °C. Yield: 20%. The thermal instability prevented the obtaining of satisfactory analytical data; however, an Fe:P ratio of 1:2 was confirmed. IR (KBr):  $\nu$  2950 s, 2920 s, 2870 s. MS (60 °C):  $m/e$  456 ( $M^+$ ), 332 ( $M^+ - C_9H_{10}$ ).

**( $\eta^2:\eta^2$ -1,5-Hexadiene)Fe( $Pr_2PC_4H_8P^iPr_2$ ) (11)** was prepared as described above by reacting  $FeCl_2 \cdot nTHF$  ( $n = 1.43$ ) with bis(diisopropylphosphino)butane, 1,5-hexadiene, and active Mg in THF at  $-35$  °C. The compound is a green solid which decomposes above  $-10$  °C. Yield: 81%. Anal. Calcd for  $C_{22}H_{46}FeP_2$ : C, 61.7; H, 10.8; Fe, 13.0; P, 14.5. Found: C, 60.9; H, 10.5; Fe, 13.4; P, 13.8. IR (KBr):  $\nu$  2955 s, 2925 s, 2890 s, 2870 s. MS (90 °C):  $m/e$  428 ( $M^+$ ), 346 ( $M^+ - C_6H_{10}$ ), 304, 262.

**( $\eta^2:\eta^2$ -1,5-Hexadiene)Fe( $Bu_2PC_2H_4P^tBu_2$ ) (13)** was prepared as described above by reacting  $FeCl_2 \cdot nTHF$  ( $n = 1.5$ ) with bis(di-*tert*-butylphosphino)ethane, 1,5-hexadiene, and active Mg in THF at  $-35$  °C. The compound is dark green and decomposes above 0 °C. Yield: 46%. Anal. Calcd for  $C_{24}H_{50}FeP_2$ : C, 63.2; H, 11.0; Fe, 12.2; P, 13.6. Found: C, 63.1; H, 10.0; Fe, 12.4; P, 13.6. IR (KBr):  $\nu$  1475 m, 1385 m, 1365 m, 1175 m, 1020 m, 845 m, 810 m, 770 m, 650 m, 640 m. MS (70 °C):  $m/e$  456 ( $M^+$ ), 374 ( $M^+ - C_6H_{10}$ ).

**( $\eta^2:\eta^2$ -1,5-Hexadiene)Fe( $PEt_3$ )<sub>2</sub> (14)** was prepared as described above by reacting  $FeCl_2 \cdot nTHF$  ( $n = 1.38$ ) with triethylphosphine, 1,5-hexadiene, and active Mg in THF at  $-35$  °C. The compound is dark violet-black. Yield: 82%. Anal. Calcd for  $C_{18}H_{40}FeP_2$ : C, 57.8; H, 10.8; Fe, 14.9; P, 16.6. Found: C, 57.6; H, 10.6; Fe, 15.0; P, 16.7. IR (KBr):  $\nu$  1460 m, 1420 m, 1375 m, 1030 m, 760 s, 695 m. MS (30 °C):  $m/e$  374 ( $M^+$ ), 292 ( $M^+ - C_6H_{10}$ ), 264 ( $M^+ - C_6H_{10}/C_2H_4$ ), 256 ( $M^+ - PEt_3$ ). Crystal structure: see Figure 2.

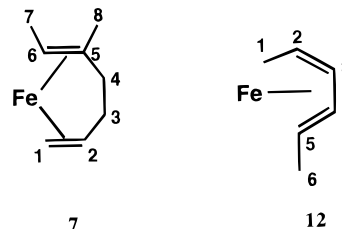
**( $\eta^2:\eta^2$ -3-Methyl-1,6-heptadiene)Fe( $Pr_2PC_2H_4P^iPr_2$ ) (6)**. The compound was prepared as described above by reacting  $FeCl_2 \cdot nTHF$  ( $n = 1.50$ ) with bis(diisopropylphosphino)ethane, 3-methyl-1,6-heptadiene, and active Mg in THF at  $-30$  °C. The compound is formed as a dark green solid which decomposes rapidly above 0 °C. Yield: 68.3%. Anal. Calcd for  $C_{22}H_{46}FeP_2$ : C, 61.7; H, 10.8; Fe, 13.0; P, 14.5. Found: C, 61.8; H, 10.8; Fe, 12.8; P, 14.6. IR (KBr):  $\nu$ (=CH) 3040 w. MS (40 °C):  $m/e$  428 ( $M^+$ ), 318 ( $M^+ - C_8H_{14}$ ).

**Reaction of 8 with CO.** Compound **8** (0.35 g, 0.8 mmol) was dissolved in pentane (40 mL) at  $-30$  °C and treated with excess CO. The solution changed from dark green to yellow. The solvent was removed at room temperature and the resulting yellow-brown, oily residue dissolved in pentane (2 mL). The solution was filtered and evaporated to give the product as a yellow, viscous oil. The spectroscopic data indicate that a mixture of isomers is formed. Yield: 0.31 g (85%). Anal. Calcd for  $C_{23}H_{46}FeOP_2$ : C, 60.5; H, 10.2; Fe, 12.2; P, 13.6. Found: C, 60.3; H, 10.2; Fe, 12.3; P, 13.7. IR (KBr):  $\nu$ (CO) 1965 s, 1905 s, 1870 s, 1815 s. MS (40 °C):  $m/e$  456 ( $M^+$ ), 428 ( $M^+ - CO$ ), 360 ( $M^+ - C_7H_{12}$ ), 332 ( $M^+ - CO/C_7H_{12}$ ).  $^1H$  NMR ( $d_8$ -toluene):  $\delta$  5.0–4.5/2.46 to  $-0.2$ .  $^{13}C$  NMR ( $d_8$ -toluene):  $\delta$  200.4 (s, CO), 89–79/58–55/39–14.  $^{31}P$  NMR ( $d_8$ -toluene):  $\delta$  70.0–51.9.

**Reaction of 10 with CO.** Compound **10** was reacted with CO in pentane at  $-30$  °C as described above to give a yellow viscous oil. The spectroscopic data indicate that a mixture of two compounds is formed. The yield is quantitative. Anal. Calcd for  $C_{25}H_{50}FeOP_2$ : C, 62.0; H, 10.4; Fe, 11.5; P, 12.8. Found: C, 61.9; H, 10.4; Fe, 11.7; P, 12.7. IR (KBr):  $\nu$ (CO) 1905 w, 1870 s. MS (65 °C):  $m/e$  484 ( $M^+$ ), 456 ( $M^+ - CO$ ), 360 ( $M^+ - C_9H_{16}$ ), 332 ( $M^+ - CO/C_9H_{16}$ ).  $^1H$  NMR ( $d_8$ -toluene):  $\delta$  ca. 4.6/2.4 to  $-0.6$ .  $^{13}C$  NMR ( $d_8$ -toluene):  $\delta$  85–76/56–50/38–14.  $^{31}P$  NMR ( $d_8$ -toluene):  $\delta$  59.4, 56.7,  $J(P,P) = 6.0$  (compound I, 20%); 56.9, 53.0,  $J(P,P) = 9.4$  (compound II, 66%).

**Reaction of 11 with CO.** Compound **11** was reacted in toluene with CO at  $-30$  °C as described above to give

( $\eta^4$ -2*Z*,4*E*)-hexadiene)Fe( $Pr_2PC_4H_8P^iPr_2$ )CO (**12**) as a yellow powder which is stable at room temperature. Yield: 23.5%. Anal. Calcd for  $C_{23}H_{46}FeOP_2$ : C, 60.5; H, 10.2; Fe, 12.2; P, 13.6. Found: C, 60.0; H, 9.9; Fe, 11.9; P, 13.3. IR (KBr):  $\nu$ (CO) 1870 vs. MS (80 °C):  $m/e$  456 ( $M^+$ ), 428 ( $M^+ - CO$ ), 374 ( $M^+ - C_6H_{10}$ ), 346 ( $M^+ - C_6H_{10}/CO$ ).  $^1H$  NMR ( $d_8$ -toluene,  $-30$  °C):  $\delta$  5.13 (m, H-3), 4.49 (m, H-4), 1.54 (d, H-6,  $J(5,6) = 5.6$ ), 1.36 (d, H-1,  $J(1,2) = 6.4$ ), 0.11 (m, H-2),  $-0.05$  (m, H-5).  $^{13}C$  NMR ( $d_8$ -toluene,  $-30$  °C):  $\delta$  223.4 (FeCO), 83.7 (C-3,  $J(C,H) = 159$ ), 77.5 (C-4,  $J(C,H) = 161$ ), 49.7 (C-2,  $J(C,H) = 152$ ),  $J(P,C) = 6.4$ ), 41.9 (C-5,  $J(C,H) = 153$ ),  $J(P,C) = 7.6(11.5)$ , 21.9 (C-6,  $J(P,C) = 4.8$ ), 17.3 (C-1,  $J(P,C) = 3.7$ ), 33.6–26.4/28.3–23.5/20.8–19.0 ( $Pr_2PC_4H_8P^iPr_2$ ).  $^{31}P$  NMR ( $d_8$ -toluene,  $-30$  °C):  $\delta$  61.3, 58.0,  $J(P,P) = 10.9$  (numbering scheme is given below; only the main isomer (80%,  $^{31}P$  NMR) has been identified).



**Reaction of 13 with CO.** Compound **13** was reacted as described above with CO in pentane at  $-30$  °C to give  $(OC)_3Fe$ ( $Bu_2PC_2H_4P^tBu_2$ ) as an almost colorless solid. Yield: 55%. Anal. Calcd for  $C_{21}H_{40}FeO_3P_2$ : C, 55.0; H, 8.8; Fe, 12.2; P, 13.0. Found: C, 54.1; H, 8.7; Fe, 12.5; P, 13.2. IR (KBr):  $\nu$ (CO) 1955 s, 1860 vs. MS (80 °C):  $m/e$  458 ( $M^+$ ), 430 ( $M^+ - CO$ ), 402 ( $M^+ - 2CO$ ), 374 ( $M^+ - 3CO$ ).  $^1H$  NMR ( $d_8$ -toluene):  $\delta$  1.39 (d,  $CH_2$ ,  $J(P,H) = 14.0$ ), 1.17 (d, Me,  $J(P,H) = 12.0$ ).  $^{13}C$  NMR ( $d_8$ -toluene):  $\delta$  37.7/30.5 ( $tBu$ ), 24.1 ( $CH_2$ ).  $^{31}P$  NMR ( $d_8$ -toluene):  $\delta$  132.6.

**Reaction of 6 with CO.** Compound **6** was reacted with CO in pentane at  $-30$  °C as described above to give an oily yellow product in quantitative yield which was shown by  $^{31}P$  NMR to consist mainly (44%) of ( $\eta^2:\eta^2$ -5-methyl-1,5-heptadiene)Fe( $Pr_2PC_2H_4P^iPr_2$ )CO (**7**). Anal. Calcd for  $C_{23}H_{46}FeOP_2$ : C, 60.5; H, 10.2; Fe, 12.2; P, 13.6. Found: C, 60.4; H, 10.2; Fe, 12.4; P, 13.5. IR (KBr):  $\nu$ (CO) 1975 w, 1870 br s. MS (60 °C):  $m/e$  456 ( $M^+$ ), 428 ( $M^+ - CO$ ), 346 ( $M^+ - C_8H_{14}$ ), 318 ( $M^+ - CO/C_8H_{14}$ ).  $^1H$  NMR ( $d_8$ -toluene):  $\delta$  4.94 (m, H-2), 3.45/3.08 (m, H-3/4),  $-0.34$  (m, H-6),  $-1.18$  (m, H-1*Z*).  $^{13}C$  NMR ( $d_8$ -toluene):  $\delta$  219.1 (FeCO), 98.0 (C-5), 77.7 (C-2), 51.1 (C-6,  $J(P,C) = 5.0/10.1$ ), 39.2 (C-4), 36.3 (C-3), 34.2 (C-1,  $J(P,C) = 7.8/12.2$ , assignment provisional).  $^{31}P$  NMR ( $d_8$ -toluene):  $\delta$  95.7, 54.4,  $J(P,P) = 40.7$  (44%) (numbering scheme is given above). The  $^{31}P$  NMR spectrum indicates the presence of two other species:  $\delta$  104.2, 98.4,  $J(P,P) = 11.5$  (23%); 98.5, 97.7,  $J(P,P) = 18.2$  (22%).

**Extended Hückel Calculations.** The EHT calculations<sup>12</sup> were based on crystal structure and valence force field modeled structures using the program ICON (version 8, 1974) and a Micro VAX II computer system. The s and p AO's (Slater type) of the C, H, Fe, and P atoms were calculated with the Coulomb potentials (IE),  $\zeta$  values, and Hückel coefficients ( $c_i$ ) shown in Table 4. The Fe d orbitals are of the double- $\zeta$  type.<sup>13</sup> The Cartesian coordinates for the atomic positions were determined from crystal structure data and modeled structures using the

Table 4

atom	IEs, eV	$\zeta_s$	IE <sub>p</sub> , eV	$\zeta_p$	IE <sub>d</sub> , eV	$\zeta_d$	$c_i^a$
H	-13.6	1.3					
C	-21.4	1.625	-11.4	1.625			
P	-18.6	1.600	-14.0	1.600			
Fe	-9.10	1.575	-5.32	0.975	-12.60	5.35	0.5366
						1.80	0.6678

$$^a \psi_d = c_1\phi(\zeta_1) + c_2\phi(\zeta_2).$$



**Table 5. Crystallographic Data for 8 and 14**

	<b>8</b>	<b>14</b>
empirical formula	C <sub>22</sub> H <sub>46</sub> FeP <sub>2</sub>	C <sub>18</sub> H <sub>40</sub> FeP <sub>2</sub>
mol wt	428.4	374.3
cryst color	black	black
cryst size, mm	0.32 × 0.49 × 0.49	0.46 × 0.42 × 0.56
a, Å	22.489(8)	9.164(7)
b, Å	15.388(3)	14.396(9)
c, Å	18.536(7)	16.035(7)
β, deg	132.53(2)	92.75(4)
V, Å <sup>3</sup>	4727.3(3)	2112.9(2)
D <sub>calcd</sub> , g cm <sup>-3</sup>	1.20	1.18
T, °C	-173	-173
λ(Mo), Å	0.710 69	0.710 69
space group (No.)	C2/c (15)	P2 <sub>1</sub> /n (14)
Z	8	4
μ <sub>abs</sub> , cm <sup>-1</sup>	7.74	8.60
no. of rflns, measd	5551 (±h,±k,±l)	6333 (±h,±k,±l)
no. of indep rflns	5383	6129
no. of obsd rflns (I > 2σ(I))	4908	4908
no. of variables	196	350
wR1 (obsd)	0.050	0.045
wR2 (obsd)	0.125	0.127
weighting factors <sup>a</sup>	a = 0.046, b = 23.860	a = 0.0905, b = 1.2173
max Δ/σ	0.001	0.001
rest electron dens, e Å <sup>-3</sup>	0.92	0.60

<sup>a</sup> Structures were refined using all data, where the function minimized was  $\sum[w(F_o^2 - F_c^2)^2]$ , with  $w^{-1} = [\sigma^2(F_o^2) + (aP)^2 + bP]$  and  $P = [\max(F_o^2, 0) + 2F_c^2]/3$ .

routine QCPE from SYBYL.<sup>14</sup> The distorted-tetrahedral (diene)Fe(bisphosphine) complexes were so oriented that one P atom occupies the basis position (0, 0, 0), the second P atom lies on the x axis, and the Fe atom lies in the x,y plane. The

octahedral complex ( $\eta^5$ -2,4-hexadien-1-yl)Fe(<sup>i</sup>Pr<sub>2</sub>PC<sub>2</sub>H<sub>4</sub>P<sup>i</sup>Pr<sub>2</sub>) was oriented with the Fe atom in the 0, 0, 0 position and the P atoms on the x axis and in the x,y plane. The calculations were simplified by replacing the alkyl groups in the bisphosphine by H atoms and the Et groups in PEt<sub>3</sub> complexes by Me groups. No attempt was made to optimize the geometry.

**Crystal Structure Determinations of 8 and 14.** Low-temperature data sets were collected with crystals mounted in Lindemann glass capillaries under argon and cooled by a cold stream of N<sub>2</sub> gas on an Enraf-Nonius CAD-4 diffractometer using graphite-monochromated Mo Kα X-radiation. Crystal data and details of data collection and structure refinement are given in Table 5. Structures were solved using the program SHELXS-86<sup>15</sup> and refined on F<sup>2</sup> using all the data (SHELXL-93).<sup>16</sup> For **8** the atoms C16, C17, C19, C21, and C22 were disordered over two positions (A:B = 0.75:0.25 occupancy), and all C atoms in the heptadiene were refined with isotropic atomic displacement parameters. All other non-H atoms were refined anisotropically while the H atoms were calculated and allowed to ride.

**Supporting Information Available:** Two X-ray crystallographic files (for **8** and **14**), in CIF format, are available. Access information is given on any current masthead page.

OM9610004

(12) Hoffmann, R. *J. Chem. Phys.* **1963**, *39*, 1397. Hoffmann, R.; Lipscomb, W. N. *J. Chem. Phys.* **1962**, *36*, 2176.

(13) Richardson, J. W.; Nieuwport, W. C.; Powell, R. R.; Edgell, L. F. *J. Chem. Phys.* **1962**, *36*, 1057.

(14) SYBYL 6.0 and 6.2, TRIPOS Associates, Inc., St. Louis, MO.

(15) Sheldrick, G. M. SHELXS 86, Program for the Solution of Crystal Structures; University of Göttingen, Göttingen, Germany, 1986.

(16) Sheldrick, G. M. *Acta Crystallogr.* **1990**, *A46*, 467.